HHS Public Access

Author manuscript

Int J Pharm. Author manuscript; available in PMC 2020 May 27.

Published in final edited form as:

Int J Pharm. 2018 July 30; 546(1-2): 1–9. doi:10.1016/j.ijpharm.2018.05.011.

Application of an Inline Dry Powder Inhaler to Deliver High Dose Pharmaceutical Aerosols during Low Flow Nasal Cannula Therapy

Dale Farkas[1], **Michael Hindle**[2], **P. Worth Longest**[1,2,*]

[1]Department of Mechanical and Nuclear Engineering, Virginia Commonwealth University, Richmond, VA

[2]Department of Pharmaceutics, Virginia Commonwealth University, Richmond, VA

Abstract

Inline dry powder inhalers (DPIs) offer a potentially effective option to deliver high dose inhaled medications simultaneously with mechanical ventilation. The objective of this study was to develop an inline DPI that is actuated using a low volume of air (LV-DPI) to efficiently deliver pharmaceutical aerosols during low flow nasal cannula (LFNC) therapy. A characteristic feature of the new inline LV-DPIs was the use of hollow capillary tubes that both pierced the capsule and provided a pathway for inlet air and exiting aerosol. Aerosolization characteristics, LFNC depositional losses and emitted dose (ED) were determined using 10 mg powder masses of a small-particle excipient enhanced growth (EEG) formulation. While increasing the number of inlet capillaries from one to three did not improve performance, retracting the inlet and outlet capillaries did improve ED by over 30%. It was theorized that high quality performance requires both high turbulent energy to deaggregate the powder and high wall shear stresses to minimize capsule retention. Best case performance included a device ED of approximately 85% (of loaded dose) and device emitted mass median aerodynamic diameter of 1.77 μm. Maximum ED through the LFNC system and small diameter (4 mm) nasal cannula was approximately 65% of the loaded dose. Potential applications of this device include the delivery of high dose inhaled medications such as surfactants, antibiotics, mucolytics, and anti-inflammatories.

Keywords

High efficiency DPI; inline DPI; active DPI; nose-to-lung aerosol delivery; pediatric aerosol delivery; low flow oxygen nasal cannula; high dose inhaled medications

[*]Corresponding author: Dr. P. Worth Longest, PhD, Virginia Commonwealth University, 401 West Main Street, P.O. Box 843015, Richmond, VA 23284-3015, Phone: (804)-827-7023, Fax: (804)-827-7030, pwlongest@vcu.edu.

Author Disclosure Statement

Virginia Commonwealth University is currently pursuing patent protection of EEG aerosol delivery, LV-DPI aerosol generation devices and patient interfaces, which if licensed, may provide a future financial interest to the authors.

1. Introduction

Inline dry powder inhalers (DPIs) create a pharmaceutical aerosol using a gas stream supplied from a positive pressure source, such as an air-filled syringe or manual ventilation bag (Behara et al., 2014; Everard et al., 1996; Laube et al., 2012; Longest et al., 2015; Pornputtapitak et al., 2014). Advantages of these devices compared with conventional inhalation driven DPIs include high quality aerosol generation (Behara et al., 2014), use in subjects that cannot generate sufficient inspiratory flow (Laube et al., 2012), reproducible aerosol delivery (Longest et al., 2015), and assistance with deep inspiration and breath hold (Tang et al., 2011). As aerosol generation is not dependent on patient inspiratory effort and following inspiration instructions, inline devices may be useful for administering aerosols to infants and young children (Laube et al., 2012; Pohlmann et al., 2013). Based on operation with a positive pressure gas source, these devices can also be used to administer aerosols during invasive and non-invasive ventilation (Everard et al., 1996; Longest et al., 2015; Tang et al., 2011).

A vast majority of studies considering aerosol delivery during mechanical ventilation have implemented nebulizers and metered dose inhalers (Ari and Fink, 2012; Dhand, 2008, 2012; Hess, 2015; Miller et al., 2003). In contrast, few studies have considered DPI delivery during mechanical ventilation (Everard et al., 1996; Tang et al., 2011; Walenga et al., 2017). This limited use may be because of the perception that humidity in the ventilation system will degrade the powder quality and aerosolization performance (Dhand, 2005). However, successful inline DPI devices for use with humidified systems have separated the humidified ventilation and DPI actuation gas streams (Walenga et al., 2017). This approach enables the implementation of DPIs in mechanical ventilation systems, with the associated advantages of rapid dose delivery, capability to administer high dose inhaled medications, reduced expense compared with many nebulizer systems, and the ability to use stable well established drug formulations.

Everard et al. (1996) published one of the first successful studies of a DPI used in a mechanical ventilation system. In this study, the budesonide Turbohaler was placed in an airtight container with an air inlet from a mechanical ventilation bag and an aerosol outlet leading to a 9 mm endotracheal tube (ETT). Under adult ventilation conditions, 20% of the initial drug mass was delivered to the end of the ETT. Pornputtapitak et al. (2014) aerosolized nanoclusters of budesonide nanoparticles using a positive pressure inline device positioned between a mechanical ventilator Y-connector and ETT. The emitted dose fraction for one way flow was 65%, but was decreased as relative humidity (RH) increased to a clinically used value. Tang et al. (2011) used a containment chamber and the Osmohaler actuated with a mechanical ventilation bag to aerosolize mannitol powder. Delivery efficiencies to the end of adult tracheal tubes were approximately 50–60% of the loaded dose. Feng et al. (2017) adapted this system for operation with airflow from a mechanical ventilator by bypassing the humidifier with a three-way valve resulting in a delivery efficiency of approximately 25% of the loaded powder mass from the end of an ETT. Our group has proposed an inline DPI actuated with a manual ventilation bag that employs excipient enhanced growth (EEG) spray dried aerosol formulations (Son et al., 2013a; Son et al., 2013b) and a 3D rod array structure (Longest et al., 2013b) to maximize aerosol

dispersion (Behara et al., 2014; Longest et al., 2014b; Longest et al., 2015). Behara et al. (2014) demonstrated that this device produced a high quality aerosol with best case mass median aerodynamic diameter (MMAD) less than 1.5 μm and device emitted doses (ED) greater than 70%. *In vitro* estimated lung delivery efficiency as a fraction of capsule loaded dose was >60% for a nasal cannula interface (Longest et al., 2015) and 80–90% for use with a noninvasive positive pressure ventilation mask (Walenga et al., 2017).

Low flow oxygen nasal cannula therapy, or LFNC therapy, is a common treatment that delivers oxygen to the nasal cavity at gas flow rates up to ~8 LPM in adults and ~1 LPM in children to treat hypoxemia (Ward, 2013). With LFNC therapy, the ventilation gas is typically not heated or humidified to maintain system simplicity and the flow rate remains low to avoid nasal discomfort associated with cold temperature and drying. To remain unobtrusive, small diameter tubing and small nasal cannula bore sizes are used, typically with internal diameters (IDs) in the range of 2–4 mm. Patients receiving LFNC therapy and other forms of noninvasive ventilation often require pharmaceutical aerosols for the treatment of underlying lung conditions. Simultaneous administration of a pharmaceutical aerosol through noninvasive ventilation systems and into the lungs (nose-to-lung or N2L delivery) is viewed as convenient and prevents the removal of ventilator support during aerosol delivery (Bhashyam et al., 2008; Dhand, 2012; Hess, 2007). However, aerosol delivery efficiency through small diameter tubing and cannula systems is known to be very low, with typical values in the range of 0.6 – 2.5% even at flow rates of 2 – 5 L/min (LPM) (Perry et al., 2013; Sunbul et al., 2014).

Based on previous studies, a number of factors are expected to significantly improve aerosol delivery efficiency during LFNC therapy and noninvasive ventilation in general. Small particle pharmaceutical aerosols have been shown to effectively penetrate nasal cannula systems and enable efficient N2L delivery (Golshahi et al., 2014a; Golshahi et al., 2013; Golshahi et al., 2014b; Longest et al., 2013c; Zeman et al., 2017). It was previously demonstrated that “streamlined” ventilation components can significantly improve the penetration of pharmaceutical aerosols, especially in nasal cannula systems for N2L delivery (Longest et al., 2014b; Longest et al., 2013a; Longest et al., 2013c). For an inline DPI, a small amount of air volume should be used to generate the aerosol as higher air flows will create impaction in the small diameter tubing and potentially exceed the subject’s inhalation flow rate. Finally, the aerosol should be created in short bursts to enable synchronization with inhalation and maximize the probability of the aerosol entering the lungs. Previously proposed inline DPI and nasal cannula systems can satisfy some of these requirements (Behara et al., 2014). However, the relatively large gas volumes (~1 L) that are used with these DPIs may prevent their effective use in the LFNC system without significant efforts to limit and synchronize aerosol formation time with inspiration.

As an alternative to inline DPIs actuated with large volumes of gas, our group has recently proposed a low gas volume (LV) DPI design that operates on approximately 10 ml of room air per actuation (Farkas et al., 2017). In this design, hollow capillary tubes are used to pierce the capsule containing the powder and form a continuous flow passage through the LV-DPI. As a result, the entire 10 ml of actuation air passes through the device and capsule to form the aerosol. Air jets formed by the capillaries inside the capsule create significant

turbulence and deaggregate the powder. A simple syringe with a luer-lock connector filled with room air was used to provide the 10 ml actuations and was manually compressed in approximately 0.2 s resulting in a short burst of 3 LPM flow. A straight-through gas flow-path design, with inlet and outlet capillaries on opposite ends of the capsule together with an EEG powder formulation produced a DPI emitted dose of 62%, mass median aerodynamic diameter (MMAD) of 1.6 μm and a fine particle fraction (FPF) less than 5 μm of 95.2%. Based on device attributes, the LV-DPI is expected to perform well in delivering aerosol during LFNC. Specifically, the small aerosol size should effectively penetrate the small diameter nasal cannula. The LV-DPI flow rate of 3 LPM is not expected to interfere with gas delivery or cause excessive deposition in the LFNC system. Finally, the very rapid aerosol generation should enable effective synchronization with inspiratory flow.

The objective of this study was to develop an inline DPI that requires low air volume (LV-DPI) to efficiently deliver pharmaceutical aerosols to adults during LFNC therapy. Devices were produced with 3D printing and evaluated in terms of regional deposition, emitted drug fraction and aerosolization using a loaded powder mass of 10 mg. As in previous studies, high efficiency performance for the delivery of EEG formulations was defined by the production of an aerosol with the following characteristics: an MMAD of less than 1.5 μm, fine particle fraction (FPF) less than 5 μm as a percentage of ED ($FPF_{<5\mu m/ED}$) above 90%, $FPF_{<1\mu m/ED}$ above 30% and a device ED greater than 75%. To achieve this performance, the previous LV-DPI with the straight-through flow-path design was first improved to increase device emitted dose while maintaining small aerosol size. A spacer design was then developed to integrate the aerosol plume into the LFNC system with minimal aerosol loss. Finally, aerosol transmission through a complete LFNC system was considered with realistic tubing curvatures. Considering the small tubing and cannula diameters of the LFNC system, effective delivery through the cannula interface was expected to be extremely challenging. However, the small particle EEG aerosols and streamlined ventilation components should significantly improve aerosol transmission. Considering that transmission efficiency through similar small diameter nasal cannula systems under LFNC conditions is reported to be on the order of 1% and below, achieving a 60% cannula ED of the initially loaded drug powder will be a significant advancement.

2. Materials and methods

2.1. Overview

The low air volume actuated DPIs developed in this study were based on our previous work developing a LV-DPI, which was evaluated based on the aerosol characteristics at the device exit (Farkas et al., 2017). The next logical step was to integrate the LV-DPI into a system to deliver the aerosol to a human subject. LFNC therapy was selected as a challenging system for the simultaneous delivery of high dose inhaled medications. From our previous study (Farkas et al., 2017), the straight-through (ST) flow-path LV-DPI was able to produce a high quality aerosol, so this design was chosen as the starting point for continued development. Considering that the previous emitted dose from the device was 62%, further improvements were sought in this study to increase the device and cannula emitted doses. The air source for the LV-DPI was a manually operated 10 mL syringe that was threaded onto the LV-DPI

using an airtight luer-lock connection. A 3-way stopcock was attached between the syringe and the LV-DPI to prevent airflow through the device in the wrong direction while connected to the positive pressure system when the actuation syringe was refilled. Based on the previous study (Farkas et al., 2017), the optimal outlet capillary diameter selected was 0.89 mm for all cases as both the aerosol characteristics and the plume characteristics were expected to be favorable for introduction into the LFNC system. The new inline LV-DPIs were tested with an optimized EEG formulation of albuterol sulfate (AS), which was previously developed by (Son et al., 2013a), containing drug, mannitol, L-leucine and poloxamer 188 in a ratio of 30:48:20:2%w/w and was spray dried using a Büchi Nano spray dryer B-90 (Büchi Laboratory-Techniques, Flawil, Switzerland). The primary particle size of the EEG formulation was tested using a Sympatec HELOS (Sympatec GmbH, Clausthal-Zellerfeld, Germany) laser diffraction system with a ASPIROS aerosol dispersion accessory, which uses a pressure drop of 4 bar (400 kPa) to disperse a small amount of powder. Aerosol characterization from the LV-DPI systems were based on drug quantification using high performance liquid chromatography (HPLC) analysis of deposition on the various device components (LV-DPI, spacer and cannula interface), to determine the emitted dose, and by cascade impaction using the Next Generation Impactor (NGI), to determine the fine particle fraction and MMAD. Further details of the devices, formulation and characterization studies are provided in the following sections.

2.2. Materials

Albuterol Sulfate (AS) USP was purchased from Spectrum Chemicals (Gardena, CA) and Pearlitol® PF-Mannitol was donated from Roquette Pharma (Lestrem, France). Poloxamer 188 (Leutrol F68) was donated from BASF Corporation (Florham Park, NJ). L-leucine and all other reagents were purchased from Sigma Chemical Co. (St. Louis, MO). Quali-V, Hydroxypropyl methylcellulose (HPMC) capsules (size 0) were donated from Qualicaps (Whitsett, NC).

A single batch of spray dried albuterol sulfate EEG formulation was produced using the optimized method described by (Son et al., 2013a). The primary particle size of the spray dried batch was determined using a laser diffraction method with a Sympatec ASPIROS dry dispersing unit and HELOS laser diffraction sensor.

2.3. Inhaler Design

The straight-through flow-path LV-DPI containing a 0.6 mm capillary inlet (0.6mm_v1) is shown in Figure 1a, while the device containing three 0.6 mm capillaries (3×0.6mm_v1) is shown in Figure 1b. The 3×0.6mm inlet was designed to have three jets of air come in contact with the powder, which was intended to reduce the amount of powder that sticks to the walls behind the inlet capillaries. The inlet and outlet capillaries were originally inserted approximately 6 mm into the capsule, which is designated as the *v1* design. After observations of where the losses were occurring in the devices, it was determined that a significant amount of the powder was depositing behind the inlet capillaries. It was expected that decreasing the insertion depth of the inlet and outlet capillaries would be beneficial, so the insertion depth was decreased as far as possible while still creating a reliable piercing of the capsule. The retraction distance was determined to be 4 mm, leaving 2 mm inserted into

the capsule. These LV-DPIs, denoted 0.6mm_v2 and 3×0.6mm_v2, are shown in Figure 1c and Figure 1d, respectively. The inlet cross sections of the v2 devices are the same as their respective v1 inlets, and images comparing the 0.6 mm and 3×0.6 mm inlet configurations are shown in Figure 1e and Figure 1f, respectively.

The inhaler designs were created using Autodesk Inventor and exported as .STL files to be prototyped. The files were then prepared using Objet Studio preparation software and were built using a Stratasys Objet24 3D Printer (Stratasys Ltd., Eden Prairie, MN) using VeroWhitePlus material at a 32 μm resolution. Support material was cleaned away from the model material using a Stratasys waterjet cleaning station and the devices were allowed to fully dry before use. The capillaries used in the LV-DPIs were custom cut from lengths of stainless steel (SAE 304) capillary tubing and were angled on one side to allow for easy piercing of the capsule upon insertion. When the capillary pierces the capsule using the single side sharpening (cf. Figure 1a inlet), a small flap of the capsule material is left hanging inside of the capsule. With the retracted outlet capillary, it was thought that this flap would cover the outlet, blocking the flow and increasing capsule retention. To prevent this blockage, the capillary was sharpened on both sides to create two smaller flaps, one on each side of the capillary (cf. Figure 1c outlet). The capillaries were then secured into place using water resistant epoxy and allowed to cure fully before use. It is noted that the sharpened capillaries were sufficiently recessed inside of the device to allow for safe operation. A rendering of the assembled 0.6mm_v2 LV-DPI is shown in Figure 2 with actuation flow moving from left to right in the figure.

2.4. Spacer Designs

The Spacer 1 design (Figure 3a) was constructed with the intent to keep the incoming ventilation gas flow separated from the aerosol plume until the plume had expanded for several centimeters. The ventilation gas flow passed through a narrow slit (~ 1 mm wide) for a distance of 10 mm in order to decrease turbulence and create a uniform velocity profile (axially symmetric in the primary direction of flow) entering the spacer near the outer wall boundary. The ventilation gas then entered a mixing chamber region, which was 25 mm in diameter and 45 mm long, next to the outer wall with the intent of inward flow motion and reducing wall deposition. The total volume of Spacer 1 was 40.4 cm^3, and it is expected that the jet exiting the LV-DPI outlet capillary into the spacer will rapidly traverse this volume. The interior walls were made as smooth as possible and all connections were streamlined to avoid unwanted powder losses.

Spacer 2, shown in Figure 3b, was designed to reduce the aerosol plume size by introducing uniform flow as soon as the aerosol exits the LV-DPI. Recirculation was believed to be responsible for a portion of the losses in the Spacer 1 design. To promote uniform flow through the spacer, a series of cylindrical rods, 1.75 mm in diameter and spaced with a 1 mm gap between the rods, was introduced to the incoming air flow. Six of these arrays were stacked together along the central axis of the spacer, in a 3D grid formation, so that each vertical array was followed by a horizontal array. Also, the vertical and horizontal arrays that make up the third and fourth set of arrays were offset so that the centers of the rods were positioned in the center of the gap of the array in front and behind that are oriented in the

same direction. Thus, from a front view the grid appears to be completely blocked. The total volume of the spacer that the aerosol traveled though was 33.7 cm^3, which was similar to the volume after the aerosol meets the airflow in Spacer 1 (33.5 cm^3). In the Spacer 2 design, the straight mixing section had a diameter and length of 30 mm and 25 mm, respectively. This mixing section then smoothly connected to a 4 mm tubing outlet over a length of 55 mm.

Both spacers consist of inlet, straight mixing, and outlet sections. These sections were connected using threaded overlaps designed and prototyped onto the pieces and sealed using two o-rings for each connection. The LV-DPIs were also connected to the spacers using a threaded connection to match the luer-lock style threads on the device outlets.

2.5. Streamlined Components

Previous studies have demonstrated that with noninvasive ventilation systems, sites of flow expansion and contraction as well as sudden direction changes were responsible for high depositional losses of aerosol (Longest et al., 2013a; Longest et al., 2013c). Our group has proposed a “streamlined” design concept in which all conduit sudden expansions and contractions were eliminated and direction changes were restricted to a minimum radius of curvature (Longest et al., 2014a; Longest et al., 2014b; Longest et al., 2013a; Longest et al., 2011). This streamlined component approach has previously shown significant increases in aerosol transmission efficiency in both high flow (Behara et al., 2014) and low flow (Longest et al., 2014b) N2L delivery systems. Based on the study of Longest et al. (2014b), an optimized streamlined nasal cannula and Y-connector were implemented in this study as shown in Figure 4. Both devices utilize 4 mm internal diameter tubing, which was consistent with the 2 – 4 mm range of commercial LFNC systems. Luer-lock style connectors were included in the connection components to facilitate assembly and disassembly of an airtight system for determining sectional aerosol deposition. These relatively bulky connectors will not be needed in a final design for clinical use.

2.6. LFNC System Setup

The 4 mm diameter tubing, shown in Figure 5, connecting the Y-connector to the cannula was ~60 cm long to simulate the length needed to curve the tubing around the ears and allow the DPI and spacer to reside sufficiently far from the patient. A simulated patient with the nasal cannula in place is shown in Figure 6a. Figure 6b shows the LV-DPI/spacer setup, while connected to ventilation gas using a standard barb fitting, and connected to the Y-connector. All tubing connections were sealed using a similar sealing system to the device, where the male connector is inserted (with two o-rings for sealing) into the corresponding female connector (either on the cannula or Y-connector) and twisted 30° to lock into place.

2.7. Evaluation of Devices, Spacers, and Full Delivery System

Aerosolization performance of the LV-DPIs was characterized using 10 mg of EEG-AS powder formulation, which was accurately weighed and manually filled into size 0 capsules. This 10 mg mass of powder filled approximately 3% of the capsule volume. It was estimated that the capsules can hold approximately 100 mg without powder contacting the capillaries when the DPI was operated in the intended horizontal position. Loaded capsules were placed

in one half of the LV-DPI and pierced when the two device halves were sealed together with a 30° turn. After the devices were assembled, a 10 mL syringe was filled with room air and then connected via the luer-lock onto a 3-way stopcock that was connected to the LV-DPI inlet. To maintain a consistent distance from the outlet of the devices to the inlet of the NGI for aerosol sizing, a custom adaptor was fabricated which held the LV-DPIs approximately 3 cm away from the NGI preseparator inlet. The powders were then aerosolized with the LV-DPI in a horizontal position. As minimal size change was expected in the aerosol under ambient temperature and relative humidity (RH) conditions, experiments were conducted with ambient air (T = 22 ± 3 °C and RH = 50 ± 5 %) with the NGI at room temperature. To allow for horizontal positioning of the inhaler, the NGI was positioned on its side (oriented vertically). The NGI was operated at 45 L/min and the preseparator and individual stages were coated with MOLYKOTE® 316 silicone spray (Dow Corning, Midland, MI) to minimize particle bounce and re-entrainment. The flowrate of 45 LPM was chosen to ensure collection of the aerosol and maintain reasonable stage cutoff diameters for evaluating a small size aerosol. To actuate the LV-DPI, the plunger of the syringe was depressed quickly (~0.2 seconds to empty) to aerosolize the powder into the inlet of the NGI. The stopcock valve was then turned to the off position for the device and the syringe was refilled with room air through the open port for a total of 5 actuations. Syringe emptying times were determined in our previous work using a single operator and high speed photography at 1000 frames/sec (Farkas et al., 2017). All measurements were made with three replicates for each design configuration.

After the best case LV-DPI was chosen, the spacer was optimized using the same device for comparison. The spacers were tested in the horizontal position using the same adapter designed to hold the device exit 3 cm away from the inlet of the NGI, as described above. After each replicate, the spacer was disassembled, and drug recovered from the sections was assayed separately. The spacer ED was defined as the percentage of the loaded dose that was not retained in both the device and spacer after 5 actuations.

For steady state testing of the full delivery system, the powder exiting the cannula was directed in the NGI while being held in place by a clamp. The cannula was not sealed to the NGI and it was expected that the NGI flow rate of 45 LPM was sufficient to capture all aerosol exiting from the cannula. A similar curvature to the tubing shown in Figure 6a was used to allow the spacer and device to be used horizontally on the benchtop. Images showing the powder exiting the cannula are shown in Figure 7 while flowing into an open environment. After testing, all of the components were disassembled and drug deposition was assayed separately with the cannula ED being defined as the percentage of the loaded dose that made it through all of the components and into the NGI.

2.8. Aerosol performance characterization methods

After aerosolization, drug masses retained in the capsule, device, spacer, and system components (tubing, Y-connector and cannula), and the drug collected on the preseparator, impaction plates and the filter of the NGI were recovered by washing with appropriate volumes of deionized water and quantified by HPLC analysis. The mass of AS retained in the capsule, device, spacer, and tubing components, determined by HPLC, was expressed as

a percentage of the loaded AS dose. AS was analyzed using a modular HPLC system (Waters Co., Milford, MA) with a Restek Allure PFP 150 × 2.1 mm column (Bellefonte, PA) connected to a 2996 PDA detector. An absorption wavelength of 276 nm was used with Empower Pro software (Waters Co., Milford, MA). The analysis was conducted using isocratic analysis with 70:30 (%v/v) methanol-20 mM ammonium formate in water (pH adjusted to 3.4 with 90% formic acid) at a flow rate of 0.4 mL/min and an injection volume of 100 μL (Behara et al., 2014; Son et al., 2013a). The LV-DPI emitted dose (LV-DPI ED) was calculated by subtracting the mass of AS retained in the capsule and device from the loaded AS dose. The spacer ED was calculated by subtracting the mass of AS retained in the capsule, device, and spacer from the loaded dose. Likewise, the cannula ED was calculated by subtracting the AS retained in all of the components from the loaded dose.

In order to determine the nominal dose of AS in the EEG-AS formulation, known masses of the formulation were dissolved in 50 ml of water and the mean amount of AS per mg of formulation was determined using HPLC analysis. For each aerosolization experiment, the measured formulation AS content and the mass of formulation loaded into the capsule was used to determine the loaded dose of AS.

The cut-off diameters of each NGI stage at the operating flow rate of 45 LPM were calculated using the formula specified in USP 35 (Chapter 601, Apparatus 5) and were used to calculate MMAD and fine particle fractions of the delivered aerosol. Fine particle fraction of the EEG formulation ($FPF_{<5\mu m/ED}$) and sub-micrometer FPF ($FPF_{<1\mu m/ED}$) were defined as the mass fractions less than 5 μm and 1 μm, respectively, expressed as a percentage of the ED. MMAD, $FPF_{<5\mu m/ED}$ and $FPF_{<1\mu m/ED}$ were calculated by linear interpolation using a plot of cumulative percentage drug mass vs. cut-off diameter.

3. Results

3.1. EEG Formulation Dispersion Characterization

The dispersion characteristics for the batch of EEG-AS formulation used in this study was determined using a Sympatec laser diffraction system using an ASPIROS/RODOS unit for comparison to previous studies as well as comparison to the aerosolization performance of the devices in this study. The geometric diameters given by the laser diffraction system were converted to aerodynamic diameters using the theoretical particle density of 1.393 g/cm^3 (Longest and Hindle, 2011). The MMAD was calculated to be 1.18 μm while the $FPF_{<5\mu m/ED}$ and $FPF_{<1\mu m/ED}$ values were found to be 100% and 38.2%, respectively. The results of this test show that the powder is highly dispersible when using a benchtop dispersion unit that operates at high pressures.

3.2. LV-DPI Optimization

Two capillary inlet configurations were tested in this study to optimize the straight-through (ST) flow-path design: an inlet containing a single 0.6 mm diameter capillary and an inlet containing three 0.6 mm capillaries spaced evenly around the long axis of the device. Performance results of the ST designs are given in Table 1. The first configuration tested was the original inlet from our previous work (Farkas et al., 2017), the single 0.6 mm inlet.

The performance, which was comparable to the previous study, included an ED of 63.1% and an MMAD of 1.56 μm. To decrease the amount of powder left in the capsule, the number of inlet capillaries was increased to three in a circular pattern around the long axis of the device. With an ED of 62.1% and MMAD of 1.66 μm, there was no significant difference found between the single and three inlet devices.

It was observed during the LV-DPI testing that powder was being lost on the inlet side of the devices, in places the jet from the inlet capillaries would not impact. To prevent this, the capillaries were retracted by no more than 4 mm to give a consistent piercing of 2 mm inside the capsule. These devices with retracted capillaries are denoted as 0.6mm_v2 and 3×0.6mm_v2. Both devices showed a significant increase in ED, with the 0.6mm_v2 device producing a mean LV-DPI ED of 84.6% and the 3×0.6mm_v2 device producing a mean LV-DPI ED of 78.1%. Both devices showed a small but significant increase in MMAD (1.77 μm for both) and a slight decrease in $FPF_{<1\mu m/ED}$ values (20%) compared to the 0.6mm_v1 device, but the ~20% higher ED (absolute difference) was considered to offset the small size increase. Because no significant differences were found between the single and triple inlet capillary LV-DPIs, the simpler of the two designs, 0.6mm_v2, was chosen as the best case for further study. Further details of device performance and statistical comparisons are provided in Table 1.

3.3. Comparison of Spacer Designs

Two spacer designs were chosen for investigation for this study with the function of controlling the aerosol plume exiting the device to allow for transport of the powder through the delivery system. Spacer 1, which is shown in Figure 3a, was designed to keep the incoming airflow separate from the aerosol plume while allowing the plume to expand. This design had a mean spacer retention of 12.2% with the MMAD increasing to 2.28 μm, which is 0.51 μm larger than the size exiting the LV-DPI device (Table 2). Corresponding $FPF_{<5\mu m/ED}$ and $FPF_{<1\mu m/ED}$ values decreased from the values leaving the LV-DPI to 89.4% and 12.2%, respectively. The second spacer design (Spacer 2), shown in Figure 3b, included six rod array inserts, each rotated 90 degrees from the next, composed of equally spaced cylindrical rods. These inserts were designed to help produce a uniform inlet airflow to help reduce losses in the spacer. In addition, this design also introduced the aerosol to the airflow as it exited from the device. This spacer saw a slight reduction in depositional losses to produce a mean spacer retention value of 9% with a similar size to Spacer 1 (MMAD = 2.31 μm) and with similar FPF values: 86.5% <5 μm and 13% <1 μm. Spacer 2 was then chosen to investigate further by connecting it to the full LFNC delivery system (Figure 5).

3.4. Effect of Flow Rate on Aerosol Characteristics

The original flow rate, 5 LPM, which was used to choose the best spacer option, served as the starting point to observe the aerosol characteristics exiting the cannula with the results given Table 3. With the best-case LV-DPI and spacer (0.6mm_v2 and Spacer 2), the mean cannula ED was 64.6% with a mean MMAD of 2.41 μm, mean $FPF_{<5\mu m/ED}$ of 84.4%, and $FPF_{<1\mu m/ED}$ of 11.3%. In an attempt to decrease either hygroscopic growth or electrostatic attraction losses of smaller particles in the very narrow tubing, which were thought to be potential sources of the size increase from the outlet of the device to the outlet of the

cannula, the flow rate was increased to 8 LPM. The increase in flow rate decreases the retention time of the powder in the system to allow either less time for hygroscopic growth or less time for the static charge to attract the small particles to the walls. The cannula ED at 8 LPM of 63.4% was not affected by the flow rate change. However, the cannula emitted size decreased significantly to 1.93 μm at 8 LPM, which provides an absolute difference of 0.48 μm (20% smaller). Fine particle fractions also increased at 8 LPM as $FPF_{<5\mu m/ED}$ was 92.4% and $FPF_{<1\mu m/ED}$ was 16.2%, indicating a smaller aerosol.

4. Discussion

Through careful optimization of the LV-DPI, device ED was increased from 62.1% to 84.6% which represents delivery of approximately 8.4 mg of formulation from the device. While the device emitted MMAD was increased to 1.77 μm, dispersion of the powder remained high with FPF values of 95.2% < 5 μm and 20.2% < 1 μm. Introduction of a new inline spacer enabled the aerosol to be combined with the LFNC delivery line with minimal loss and maintained separate ventilation and DPI actuation gas streams. Optimization of the spacer design reduced spacer loss from 12.2% (concentric design) to 9% (uniform flow design). A low total spacer volume was maintained (< 33.7 cm^3) to provide an acceptable time delay between device actuation and transmission through the nasal cannula. The aerosol exiting the nasal cannula was larger than exiting the LV-DPI device and was greater than 2 μm, which is larger than the ~1.5 μm MMAD that was desired. However, aerosol transmission efficiency out of the cannula (i.e., cannula ED) achieved the targeted >60% goal and was as high as 65% under optimized conditions.

One surprising outcome of this study was that aerosol size increased through the LFNC system resulting in a greater than 2 μm outlet MMAD at a LFNC flow rate of 5 LPM. Increasing the LFNC flow rate to 8 LPM produced approximately the same overall system depositional loss, but reduced the ex-cannula MMAD to 1.93 μm. One possible explanation of this size increase is hygroscopic growth of the EEG aerosol, which is a time dependent process (Longest and Hindle, 2012). Longer residence time with 5 LPM flow allows for more growth and a larger outlet aerosol. However, the LFNC gas is assumed to be almost completely dry. The humidity for aerosol growth would then come entirely from the 10 ml of room air injected into the system with each actuation, which seems unlikely. An alternative explanation may be aerosol charge. Dry powder aerosols are known to have an electrostatic charge, especially in dry environments (Byron et al., 1997; Kwok and Chan, 2009). Smaller particles are also likely more influenced by charge than larger particle (Vinchurkar et al., 2009). Hence, the electrostatic charge on the small particles may cause a disproportionate loss of the small particle size fraction at 5 LPM thereby increasing the overall size of the aerosol. Importantly, with either scenario, the net aerosol transmission efficiency through the cannula is high and in the range of 63–65%. If a smaller aerosol with MMAD < 2 μm is desired at the cannula outlet to minimize nasal depositional loss, then increasing the gas flow to 8 LPM for the short time of aerosol administration provides a reasonable option.

The aerosol size exiting the cannula will primarily affect nasal depositional loss (Garcia et al., 2009; Schroeter et al., 2015) as well as the final droplet size achieved by the EEG

aerosol (Longest and Hindle, 2011). The degree of nasal deposition will depend on the nasal inhalation flow rate and may be different from ambient inhaled aerosols due to the presence of the nasal cannula (Walenga et al., 2014). From previous experiments with nasal aerosols with a nasal cannula interface, depositional loss with a 2 μm particle at a nasal inhalation flow rate of 30 LPM is expected to be approximately 10% or less. As a result, the estimated lung delivery efficiency including nasal losses will be ~50–60% of the initial loaded dose. Furthermore, depending in the lung region to be targeted, it may be beneficial to start the EEG particle size at ~ 2 μm in order to achieve a larger final droplet size (Longest and Hindle, 2011; Tian et al., 2014). Based on the study of Longest and Hindle (2011), a 2 μm initial EEG particle can achieve a final size > 6 μm within the lungs.

Perhaps more important to total lung deposition than the inhaled 2 μm MMAD aerosol is the fact that the aerosol is delivered very rapidly. The transit time (the time required for the aerosol to reach the cannula after syringe actuation) of the delivery system was similar for 5 and 8 LPM and is approximately 0.2 s for both flow rates. However, delivery duration from the cannula (the duration of time that aerosol is exiting the cannula) was affected by the flow rate and at 5 and 8 LPM is approximately 0.75 and 0.5 s, respectively. This compact time window should enable actuation with the start of nasal inspiration. A simple pressure monitor or flow direction element on the cannula can be used to sense inspiratory or expiratory flow. Ideally, conscious subjects can be instructed to inhale deeply through the nose for a period up to 3 s, enabling all of the ex-cannula dose to enter the nose. Synchronization with inspiration and nasal depositional losses will be considered in future studies.

Optimization of the device in this study provided a significant improvement in ED compared with the previous LV-DPI development study (Farkas et al., 2017). The primary device change that enabled this improvement was retracting the capillaries approximately 4 mm each. Physically, this retraction maintained higher velocity near the capillary walls and prevented powder deposition near the capillary base. A slight increase in aerosol size was observed to a device outlet MMAD of 1.77 μm for the best case design. This size increase of 0.21 μm is likely due to both more of the powder being aerosolized and reduced shear forces associated with the capillary outlet positioned closer to the capsule wall. Other design improvements to increase ED were less effective. Due to no significant difference in the single (0.6 mm) and triple (3×0.6 mm) capillary inlet designs, the simpler, single 0.6 mm capillary inlet was chosen for further study. Both the optimization of the spacer and flow rate selection for cannula delivery used the same device for comparison.

Previous studies evaluating N2L aerosol delivery using small diameter cannula consistent with LFNC systems are rare. Perry et al. (2013) previously considered transmission efficiency of an Aeroneb Solo mesh nebulizer at multiple flow rates through a nasal cannula system. At an airflow rate of 5 LPM the percentage of nominal dose exiting adult, pediatric and infant small bore cannula were 2.5, 0.6 and 0.6%, respectively. The aerosol MMAD exiting the adult cannula at 5 LPM was 0.48 μm (Perry et al., 2013). Particles in the size range of 0.5 μm are expected to have limited lung deposition and be largely exhaled (Kim and Jaques, 2000). In contrast, the newly developed LV-DPI system delivered 65% of the initial dose through the cannula, resulting in a 26-fold increase compared with the

conventional mesh nebulizer system and adult cannula size of Perry et al. (2013). Furthermore, the exiting aerosol size of 2 μm and use of EEG particles are expected to enable lung targeted deposition and minimal exhaled aerosol loss (Tian et al., 2013).

Limitations of the current study include the need for additional device improvements, addition of a nasal cavity model and breathing waveform, evaluation of flow synchronization and consideration of lung deposition and exhaled dose. To aid in decreasing losses due to possible static charge on the delivery system elements, it may be necessary to use a static dissipative material for the components in the future. Inclusion of a realistic nasal airway model is needed to verify high transmission of the aerosol to the lungs. It is expected that the back pressure introduced with the spacer and nasal cannula interface marginally reduced performance. Therefore, including a breathing subject may improve cannula ED and aerosol size. Aerosol transmission measurements were made to evaluate the potential for flow synchronization. However, experiments with a breathing waveform are still needed. Finally, many studies equate tracheal filter deposition with lung deposition, which ignores the exhaled aerosol fraction. Improved lung deposition and reduced exhaled dose is expected with EEG aerosols (Tian et al., 2014), but needs to be confirmed.

5. Conclusions

In conclusion, this study has successfully improved the LV-DPI and applied the device to achieve high efficiency delivery of a high dose dry powder aerosol in a LFNC system. Device modifications were implemented to improve ED and reduce spacer depositional loss. Transmission efficiency of loaded drug mass through the optimized system was 65%, which represents a 26-fold increase compared with similar commercial systems (Perry et al., 2013). Application of this technology to other less challenging systems with larger tubing diameters will further increase transmission efficiency. A primary advantage of using a dry powder device is the large powder mass that can be administered in a short amount of time. The developed system delivered a 10 mg powder mass in approximately 38 s (assuming a 7.5 s breathing cycle for deep inspiration) compared to a minimum 7 minute with a mesh nebulizer at a 0.5% drug concentration, not accounting for system losses. Potential applications of this device include high dose inhaled medications such as inhaled surfactants, antibiotics, mucolytics, and anti-inflammatories. Further studies are needed to verify the potential for synchronization with inhalation, high lung transmission efficiency, and low exhaled dose.

Acknowledgements

Research reported in this publication was supported by the Eunice Kennedy Shriver National Institute of Child Health & Human Development of the National Institutes of Health under Award Number R01HD087339 and by the National Heart, Lung and Blood Institute of the National Institutes of Health under Award Number R01HL139673 The content is solely the responsibility of the authors and does not necessarily represent the official views of the National Institutes of Health.

References

Ari A, Fink JB, 2012 Inhalation therapy in patients receiving mechanical ventilation: an update. Journal of Aerosol Medicine and Pulmonary Drug Delivery 25, 319–332. [PubMed: 22856594]

Behara SRB, Longest PW, Farkas DR, Hindle M, 2014 Development of high efficiency ventilation bag actuated dry powder inhalers. International Journal of Pharmaceutics 465, 52–62. [PubMed: 24508552]

Bhashyam AR, Wolf MT, Marcinkowski AL, Saville A, Thomas K, Carcillo JA, Corcoran TE, 2008 Aerosol delivery through nasal cannulas: An in vitro study. Journal of Aerosol Medicine and Pulmonary Drug Delivery 21, 181–187. [PubMed: 18518794]

Byron PR, Peart J, Staniforth JN, 1997 Aerosol Electrostatics I: Properties of fine powders before and after aerosolization by dry powder inhalers. Pharmaceutical Research 14, 698–705. [PubMed: 9210184]

Dhand R, 2005 Inhalation therapy with metered-dose inhalers and dry powder inhalers in mechanically ventilated patients. Respiratory Care 50, 1331–1344. [PubMed: 16185369]

Dhand R, 2008 Aerosol delivery during mechanical ventilation: From basic techniques to new devices. Journal of Aerosol Medicine and Pulmonary Drug Delivery 21, 45–60. [PubMed: 18518831]

Dhand R, 2012 Aerosol therapy in patients receiving noninvasive positive pressure ventilation. Journal of Aerosol Medicine and Pulmonary Drug Delivery 25, 63–78. [PubMed: 22191396]

Everard ML, Devadason SG, LeSouef PN, 1996 In vitro assessment of drug delivery through an endotracheal tube using a dry powder inhaler delivery system. Thorax 51, 75–77. [PubMed: 8658374]

Farkas DR, Hindle M, Longest PW, 2017 Development of an Inline Dry Power Inhaler that Requires Low Air Volume. Journal of Aerosol Medicine and Pulmonary Drug Delivery (in press).

Feng B, Tang P, Leung SSY, Dhanani J, Chan H-K, 2017 A novel in-line delivery system to administer dry powder mannitol to mechanically ventilated patients. Journal of Aerosol Medicine and Pulmonary Drug Delivery 30, 100–107. [PubMed: 27754730]

Garcia GJM, Tewksbury EW, Wong BA, Kimbell JS, 2009 Interindividual variability in nasal filtration as a function of nasal cavity geometry. Journal of Aerosol Medicine and Pulmonary Drug Delivery 22, 1–17.

Golshahi L, Longest PW, Azimi M, Syed A, Hindle M, 2014a Intermittent aerosol delivery to the lungs during high flow nasal cannula therapy. Respiratory Care 59, 1476–1486. [PubMed: 24917454]

Golshahi L, Tian G, Azimi M, Son Y-J, Walenga RL, Longest PW, Hindle M, 2013 The use of condensational growth methods for efficient drug delivery to the lungs during noninvasive ventilation high flow therapy. Pharmaceutical Research 30, 2917–2930. [PubMed: 23801087]

Golshahi L, Walenga RL, Longest PW, Hindle M, 2014b Development of a transient flow aersol mixer-heater system for lung delivery of nasally administered aerosols using a nasal cannula. Aerosol Science and Technology 48, 1009–1021.

Hess DR, 2007 The mask of noninvasive ventilation: Principles of design and effects on aerosol delivery. Journal of Aerosol Medicine 20, S85–S99. [PubMed: 17411410]

Hess DR, 2015 Aerosol therapy during noninvasive ventilation or high-flow nasal cannula. Respiratory Care 60, 880–893. [PubMed: 26070581]

Kim CS, Jaques PA, 2000 Respiratory dose of inhaled ultrafine particles in healthy adults. Philosophical Transactions Of The Royal Society Of London Series A-Mathematical Physical And Engineering Sciences 358, 2693–2705.

Kwok PCL, Chan HK, 2009 Electrostatics of pharmaceutical inhalation aerosols. Journal Of Pharmacy And Pharmacology 61, 1587–1599. [PubMed: 19958580]

Laube BL, Sharpless G, Shermer C, Sullivan V, Powell K, 2012 Deposition of dry powder generated by solovent in Sophia Anatomical infant nose-throat (SAINT) model. Aerosol Science and Technology 46, 514–520.

Longest PW, Azimi M, Golshahi L, Hindle M, 2014a Improving Aerosol Drug Delivery During Invasive Mechanical Ventilation With Redesigned Components. Respiratory Care 59, 686. [PubMed: 24106320]

Longest PW, Behara SRB, Farkas DF, Hindle M, 2014b Efficient generation and delivery of dry powder aeorsols druing low flow oxygen administration. Drug Delivery to the Lungs - DDL 24 http://ddl-conference.com/files/DDL24Abstracts/oral/05.Hindle.pdf.

Longest PW, Golshahi L, Behara SRB, Tian G, Farkas DR, Hindle M, 2015 Efficient nose-to-lung (N2L) aerosol delivery with a dry powder inhaler. Journal of Aerosol Medicine and Pulmonary Drug Delivery 28, 189–201. [PubMed: 25192072]

Longest PW, Golshahi L, Hindle M, 2013a Improving pharmaceutical aerosol delivery during noninvasive ventilation: Effects of streamlined components. Annals of Biomedical Engineering 41, 1217–1232. [PubMed: 23423706]

Longest PW, Hindle M, 2011 Numerical model to characterize the size increase of combination drug and hygroscopic excipient nanoparticle aerosols. Aerosol Science and Technology 45, 884–899. [PubMed: 21804683]

Longest PW, Hindle M, 2012 Condensational growth of combination drug-excipient submicrometer particles: Comparison of CFD predictions with experimental results. Pharmaceutical Research 29, 707–721. [PubMed: 21948458]

Longest PW, Son Y-J, Holbrook LT, Hindle M, 2013b Aerodynamic factors responsible for the deaggregation of carrier-free drug powders to form micrometer and submicrometer aerosols. Pharmaceutical Research 30, 1608–1627. [PubMed: 23471640]

Longest PW, Tian G, Hindle M, 2011 Improving the lung delivery of nasally administered aerosols during noninvasive ventilation - An application of enhanced condensational growth (ECG). Journal of Aerosol Medicine and Pulmonary Drug Delivery 24, 103–118, DOI: 10.1089/jamp.2010.0849. [PubMed: 21410327]

Longest PW, Walenga RL, Son Y-J, Hindle M, 2013c High efficiency generation and delivery of aerosols through nasal cannula during noninvasive ventilation. Journal of Aerosol Medicine and Pulmonary Drug Delivery 26, 266–279. [PubMed: 23273243]

Miller DD, Amin MM, Palmer LB, Shah AR, Smaldone GC, 2003 Aerosol delivery and modern mechanical ventilation - In vitro/in vivo evaluation. American Journal Of Respiratory And Critical Care Medicine 168, 1205–1209. [PubMed: 12893644]

Perry SA, Kesser KC, Geller DE, Selhorst DM, Rendle JK, Hertzog JH, 2013 Influences of Cannula Size and Flow Rate on Aerosol Drug Delivery Through the Vapotherm Humidified High-Flow Nasal Cannula System. Pediatric Critical Care Medicine 14, E250–E256. [PubMed: 23628834]

Pohlmann G, Iwatschenko P, Koch W, Windt H, Rast M, Gama de Abreu M, Taut FJH, De Muynck C, 2013 A novel continuous powder aerosolizer (CPA) for inhalative administration of highly concentrated recombinant surfactant protein-C (rSP-C) surfactant to perterm neonates. Journal of Aerosol Medicine and Pulmonary Drug Delivery 26, 370–379. [PubMed: 23421901]

Pornputtapitak W, El-Gendy N, Mermis J, O'Brein-Ladner A, Berkland C, 2014 NanoCluster budesondie formulations enable efficient drug delivery driven by mechanical ventilation. International Journal of Pharmaceutics 462, 19–28. [PubMed: 24374223]

Schroeter JD, Tewksbury EW, Wong BA, Kimbell JS, 2015 Experimental measurements and computational predictions of regional particle deposition in a sectional nasal model. Journal of Aerosol Medicine and Pulmonary Drug Delivery 28, 20–29. [PubMed: 24580111]

Son Y-J, Longest PW, Hindle M, 2013a Aerosolization characteristics of dry powder inhaler formulations for the excipient enhanced growth (EEG) application: Effect of spray drying process conditions on aerosol performance. International Journal of Pharmaceutics 443, 137–145. [PubMed: 23313343]

Son Y-J, Longest PW, Tian G, Hindle M, 2013b Evaluation and modification of commercial dry powder inhalers for the aerosolization of submicrometer excipient enhanced growth (EEG) formulation. European Journal of Pharmaceutical Sciences 49, 390–399. [PubMed: 23608613]

Sunbul F, Fink JB, Harwood R, Sheard MM, Zimmerman RD, Ari A, 2014 Comparison of HFNC, bubble CPAP and SiPAP on aerosol delviery in neonates: An in-vitro study. Pediatric Pulmonology DOI 10.1002/ppul.23123.

Tang P, Chan HK, Rajbhandari D, Phipps P, 2011 Method to Introduce Mannitol Powder to Intubated Patients to Improve Sputum Clearance. Journal Of Aerosol Medicine And Pulmonary Drug Delivery 24, 1–9. [PubMed: 20961167]

Tian G, Hindle M, Longest PW, 2014 Targeted Lung Delivery of Nasally Administered Aerosols. Aerosol Science and Technology 48, 434–449. [PubMed: 24932058]

Tian G, Longest PW, Li X, Hindle M, 2013 Targeting aerosol deposition to and within the lung airways using excipient enhanced growth. Journal of Aerosol Medicine and Pulmonary Drug Delivery 26, 248–265. [PubMed: 23286828]

Vinchurkar S, Longest PW, Peart J, 2009 CFD simulations of the Andersen cascade impactor: Model development and effects of aerosol charge. Journal of Aerosol Science 40, 807–822.

Walenga RL, Longest PW, Kaviratna A, Hindle M, 2017 Aerosol drug delivery during noninvasive positive pressure ventilation: Effects of intersubject variability and excipient enhanced growth. Journal of Aerosol Medicine and Pulmonary Drug Delivery 30, 190–205. [PubMed: 28075194]

Walenga RL, Tian G, Hindle M, Yelverton J, Dodson K, Longest PW, 2014 Variability in nose-to-lung aerosol delivery. Journal of Aerosol Science 78, 11–29. [PubMed: 25308992]

Ward JJ, 2013 High-flow oxygen administration by nasal cannula for adult and perinatal patients. Respiratory Care 58, 98–120. [PubMed: 23271822]

Zeman KL, Rojas Balcazar J, Fuller F, Donn KH, Boucher RC, Bennett WD, Donaldson SH, 2017 A trans-nasal aerosol delivery device for efficient pulmonary deposition. Journal of Aerosol Medicine and Pulmonary Drug Delivery 30, 223–229. [PubMed: 28157412]

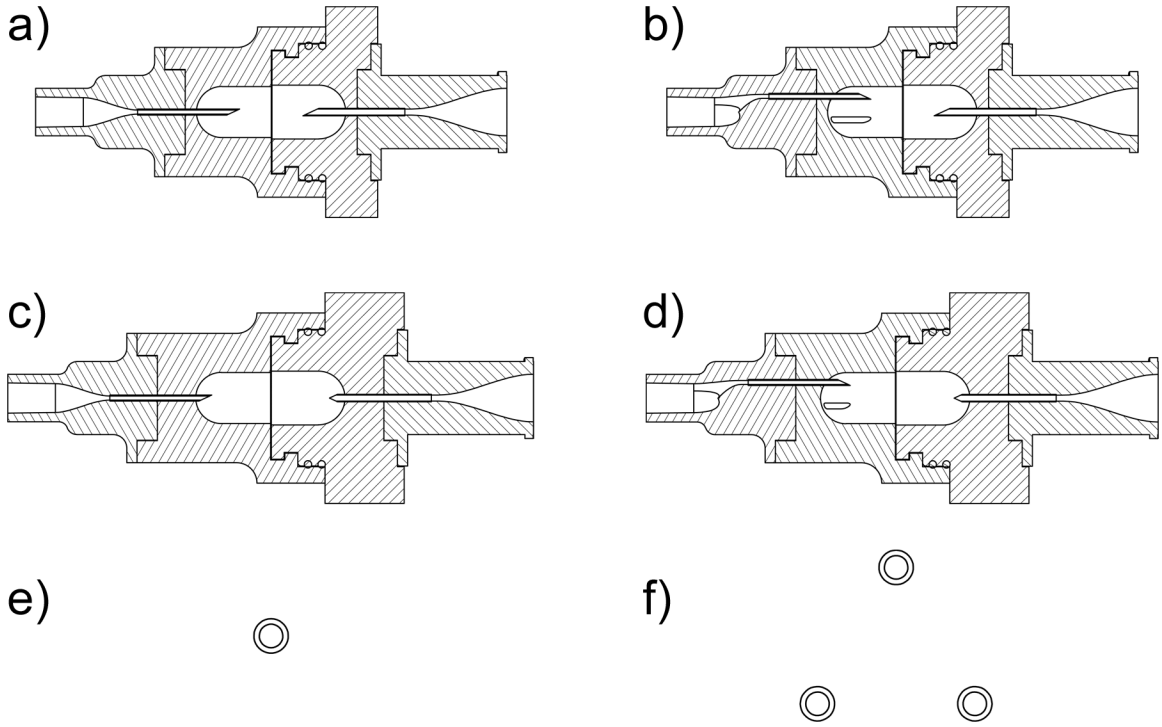

Fig. 1:

Mid-plane cross-sectional view of the LV-DPI devices with inlet (left side) and outlet (right side) capillary internal diameters: a) 0.6mm-0.89mm_v1, b) 3×0.6mm-0.89mm_v1, c) 0.6mm-0.89mm_v2, d) 3×0.6mm-0.89mm_v2; and inlet capillary patterns for the (e) single inlet and (f) three capillary inlet. The insertion depths for v1 and v2 were 6mm and 2mm, respectively.

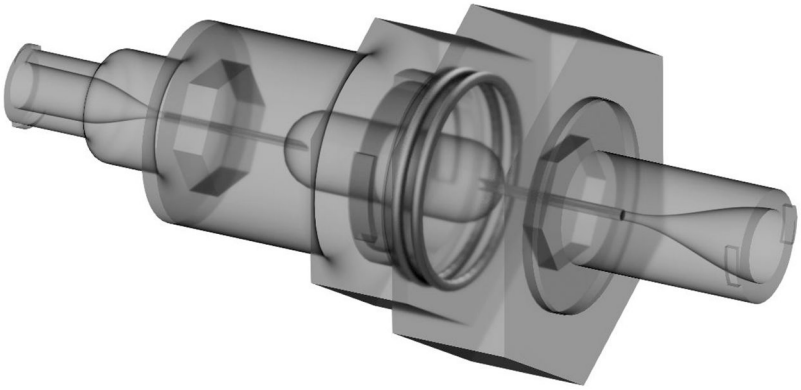

Fig. 2:
Semi-transparent 3D rendering of the 0.6mm-0.89mm_v2 (2mm needle insertion depth) device.

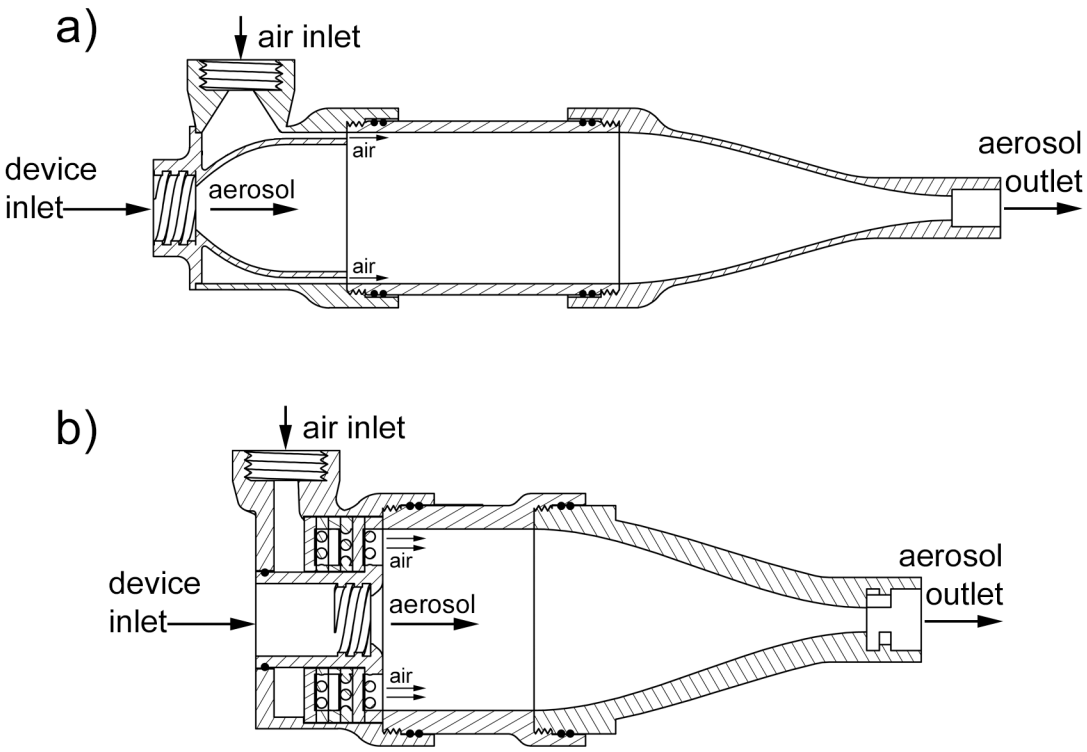

Fig. 3:
Section views of the two spacer designs: a) Spacer 1, b) Spacer 2.

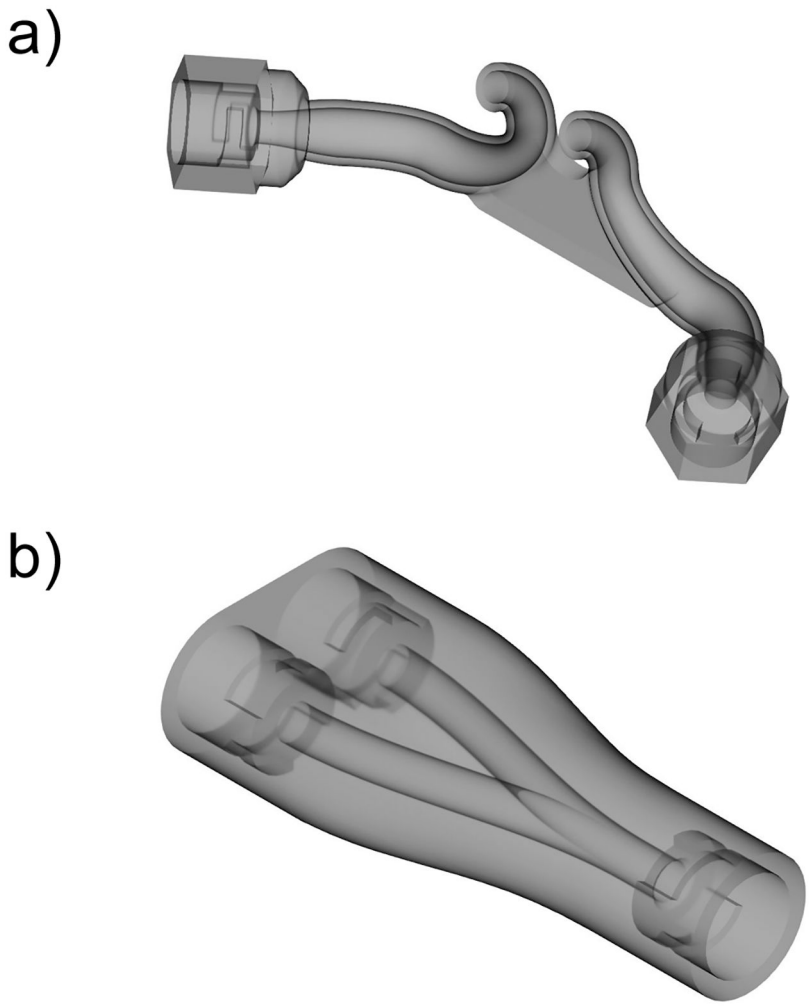

Fig. 4:
3D renderings of the streamlined components in the delivery system: a) nasal cannula, b) y-connector

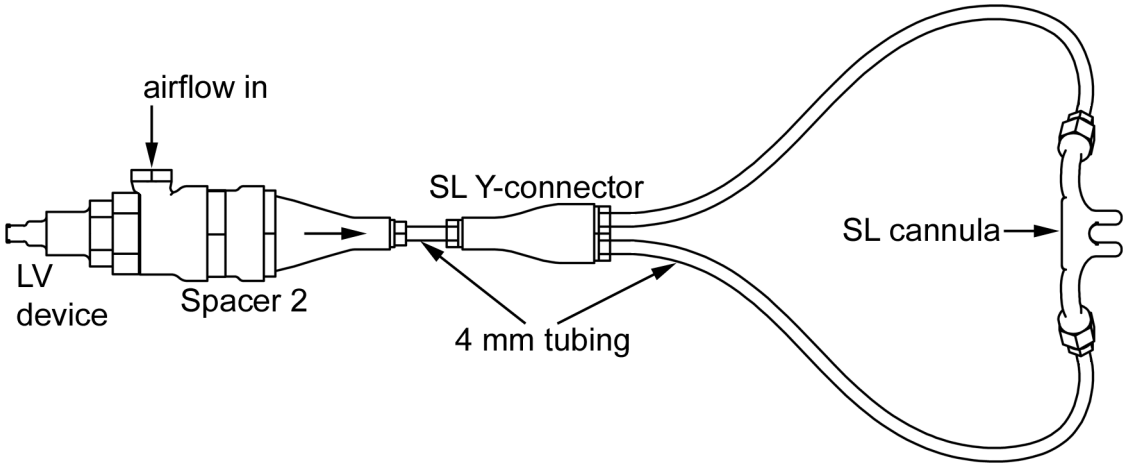

Fig. 5:
Schematic drawing showing the overall layout of the delivery system with each component labeled.

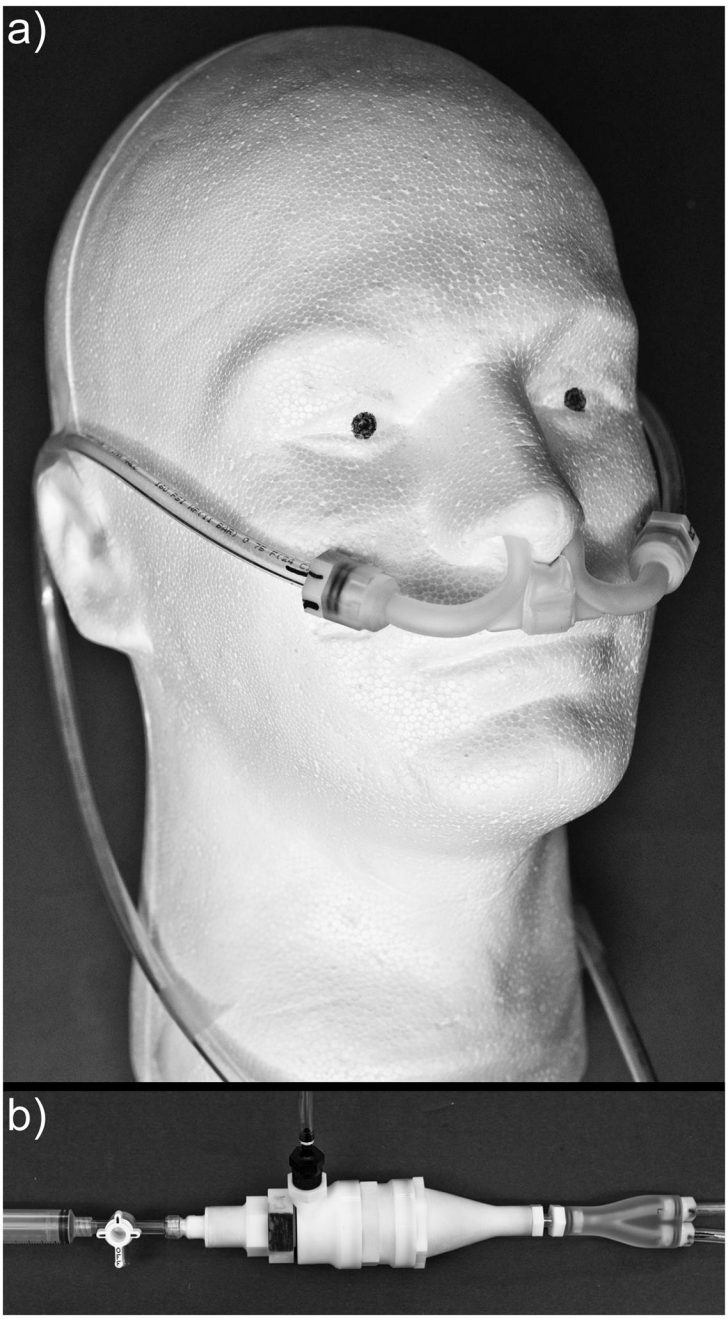

Fig. 6:

Complete LFNC plus LV-DPI delivery system: a) tubing and cannula positioned on a mannequin head, b) assembly of the syringe, device, spacer, and y-connector.

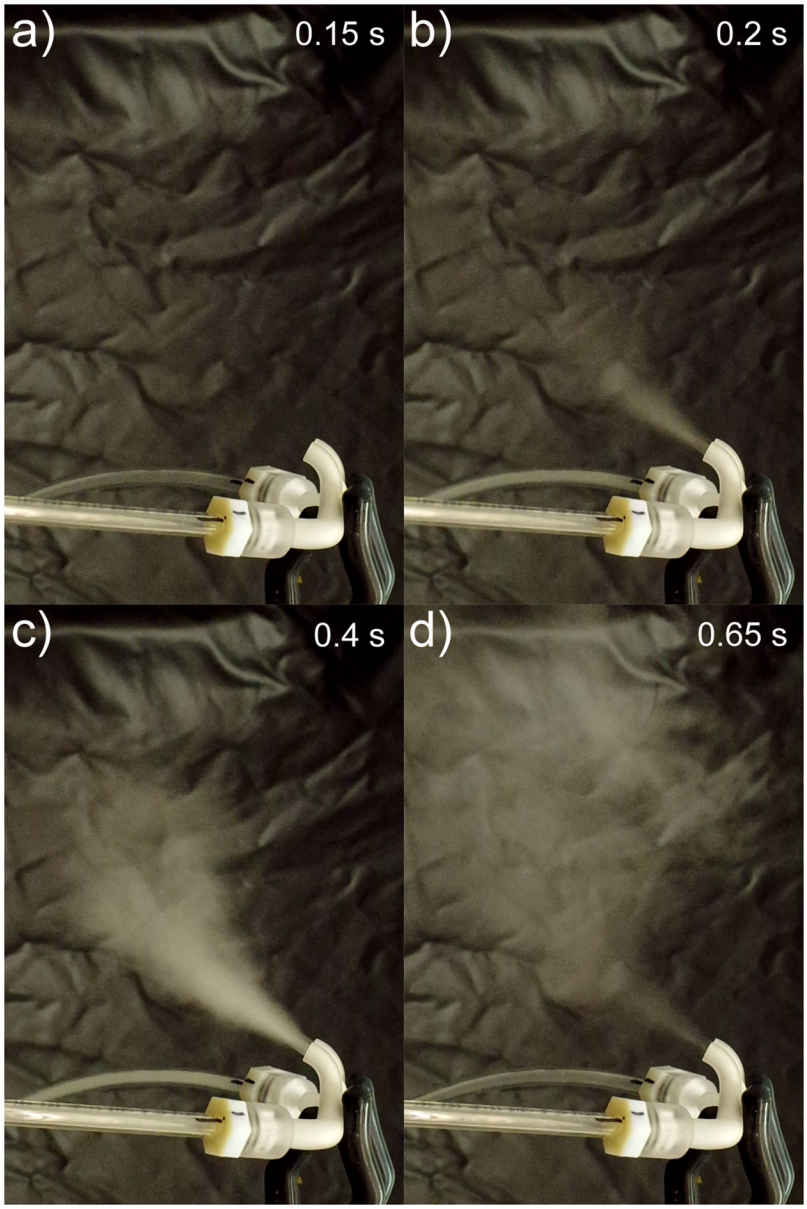

Fig. 7:

Images of powder leaving the cannula at different times during administration: a) just before powder exits, b) powder beginning to exit, c) midway through dose emission, d) end of dose emission.

Table 1:

Optimization of Straight-Through (ST) flow-path LV-DPI. Mean aerosol characteristics with standard deviations (SD) shown in parenthesis [n=3].

	Inlet Capillary Dimensions			
Description	**0.6mm_v1**	**3×0.6mm_v1**	**0.6mm_v2**	**3×0.6mm_v2**
LV-DPI ED (%) *	63.1 (4.8)	62.1 (1.5)	84.6 (6.3) **, ***	78.1 (3.0) **, ***
Capsule (%) *	30.4 (6.1)	28.6 (3.9)	14.4 (5.8) **, ***	18.7 (1.8) **, ***
LV-DPI (%) *	6.4 (3.1)	9.3 (2.5)	1.0 (0.6) ***	3.2 (1.2) ***
$FPF_{<5\mu m/ED}$ (%) *	97.8 (0.1)	95.7 (1.5)	95.2 (0.4)	93.5 (1.5) **
$FPF_{<1\mu m/ED}$ (%) *	23.9 (0.5)	21.3 (1.0)	20.2 (1.7) **	20.1 (1.0) **
MMAD (μm) *	1.56 (0.01)	1.66 (0.04)	1.77 (0.08) **	1.77 (0.03) **

* $p<0.05$ significant effect of capillary retraction on % ED, % capsule, and % LV-DPI drug retention (one-way ANOVA), together with $FPF_{<5\mu m/ED}$, $FPF_{<1\mu m/ED}$ and MMAD.

** $p<0.05$ significant difference compared to 0.6mm_v1 (post-hoc Tukey).

*** $p<0.05$ significant difference compared to 3×0.6mm_v1 (post-hoc Tukey).

Table 2:

Optimization of Spacer using the best case 0.6mm_v2 LV-DPI. Mean aerosol characteristics with standard deviations (SD) shown in parenthesis [n=3].

Description	Spacer 1	Spacer 2
Capsule (%)	10.7 (4.9)	7.6 (0.2)
LV-DPI (%)	2.2 (1.3)	1.2 (0.1)
LV-DPI ED (%)	87.1 (5.9)	91.2 (0.2)
Spacer (%)	12.2 (1.3)	9.0 (1.8) *
Spacer ED (%)	74.8 (5.8)	82.2 (1.6) *
$FPF_{<5\mu m/ED}$ (%)	89.4 (3.9)	86.5 (3.1)
$FPF_{<1\mu m/ED}$ (%)	12.2 (1.1)	13.0 (0.7)
MMAD (μm)	2.28 (0.18)	2.31 (0.11)

* $p < 0.05$ significant difference compared to Spacer 1 (t-test).

Table 3:

Comparison of entire delivery system at flow rates of 5 LPM and 8 LPM using the best case LV-DPI (0.6mm_v2) and spacer (Spacer 2). Mean aerosol characteristics with standard deviations (SD) shown in parenthesis [n=3].

Description	5 LPM	8 LPM
Capsule (%)	15.0 (2.3)	12.5 (3.3)
Device (%)	2.0 (0.2)	3.1 (0.9)
Device ED (%)	83.0 (2.1)	84.5 (2.6)
Spacer (%)	6.7 (0.3)	5.9 (1.0)
Spacer ED (%)	76.2 (1.8)	78.6 (2.7)
Y-Connector (%)	2.9 (0.6)	4.5 (1.2)
Tubing (%)	3.9 (0.7)	4.5 (1.3)
Cannula (%)	4.8 (0.7)	6.2 (3.1)
Cannula ED (%)	64.6 (1.1)	63.4 (3.1)
$FPF_{<5\mu m/ED}$ (%)	84.4 (1.8)	92.4 (3.7) *
$FPF_{<1\mu m/ED}$ (%)	11.3 (0.3)	16.2 (0.7) *
MMAD (μm)	2.41 (0.05)	1.93 (0.09) *

* $p < 0.05$ significant difference compared to 5 LPM (t-test).